Role of Poly(ADP-Ribose) Polymerase Activation in Diabetic Neuropathy

Irina G. Obrosova,[1] Fei Li,[1] Omorodola I. Abatan,[1] Mark A. Forsell,[2] Katalin Komjáti,[3] Pal Pacher,[3] Csaba Szabó,[3] and Martin J. Stevens[1]

Oxidative and nitrosative stress play a key role in the pathogenesis of diabetic neuropathy, but the mechanisms remain unidentified. Here we provide evidence that poly(ADP-ribose) polymerase (PARP) activation, a downstream effector of oxidant-induced DNA damage, is an obligatory step in functional and metabolic changes in the diabetic nerve. PARP-deficient ($PARP^{-/-}$) mice were protected from both diabetic and galactose-induced motor and sensory nerve conduction slowing and nerve energy failure that were clearly manifest in the wild-type ($PARP^{+/+}$) diabetic or galactose-fed mice. Two structurally unrelated PARP inhibitors, 3-aminobenzamide and 1,5-isoquinolinediol, reversed established nerve blood flow and conduction deficits and energy failure in streptozotocin-induced diabetic rats. Sciatic nerve immunohistochemistry revealed enhanced poly(ADP-ribosyl)ation in all experimental groups manifesting neuropathic changes. Poly(ADP-ribose) accumulation was localized in both endothelial and Schwann cells. Thus, the current work identifies PARP activation as an important mechanism in diabetic neuropathy and provides the first evidence for the potential therapeutic value of PARP inhibitors in this devastating complication of diabetes. *Diabetes* 53: 711–720, 2004

Diabetic distal symmetric sensorimotor polyneuropathy affects up to 60–70% of diabetic patients and is the leading cause of foot ulceration and amputation (1). Improved blood glucose control reduces the risk of peripheral diabetic neuropathy (PDN), thereby implicating hyperglycemia as a leading causative factor. Diabetic hyperglycemia causes PDN via several mechanisms, among which increased aldose reductase (AR) activity (2–5), nonenzymatic glycation/glycoxidation (6,7), and activation of protein kinase C (2,8) are the best studied. All three mechanisms contribute to enhanced oxidative and nitrosative stress (4,5,7,9–11) resulting from imbalance between production and neutralization of reactive oxygen species. Enhanced oxidative stress has been documented in peripheral nerve (4,5,8,12–14), dorsal root and sympathetic ganglia (15), and vasculature (16,17) of the peripheral nervous system and has been implicated in neurovascular dysfunction and motor and sensory nerve conduction velocity (MNCV and SNCV) deficits, impaired neurotrophic support, nerve metabolic and signal transduction changes, and morphologic abnormalities characteristic for diabetes (4,5,12,14,16–20). Evidence for the pathophysiologic role of reactive nitrogen species in PDN is also emerging (16,21).

The question of how oxidative and nitrosative stress causes PDN remains open. We explored the role for poly(ADP-ribose) (PAR) polymerase (PARP-1; EC 2.4.2.30), a nuclear enzyme that is activated by oxidant-induced DNA single-strand breakage and transfers ADP-ribose residues from NAD^+ to nuclear proteins (22–25). PARP-1 is present in both endothelial cells (22,23) and Schwann cells of the peripheral nerve (26). PARP-1 activation is clearly manifest in diabetes and contributes to diabetic endothelial dysfunction (22–24), an important factor in diabetic neuropathy (1). PARP activation causes profound metabolic changes (22–24) and affects gene expression (27–29). In addition, PARP is required for translocation of apoptosis-inducing factor from the mitochondria to the nucleus and thus for PARP-1–mediated programmed cell death (25) recently implicated in the pathophysiology of PDN (30). Thus, we hypothesized that PARP-1 activation triggers multiple pathogenetic mechanisms resulting from oxidative stress and is an obligatory step in the development of PDN. The test this hypothesis, we designed four specific aims: *1*) to evaluate whether PARP-1–deficient ($PARP^{-/-}$) mice are less prone to the development of diabetic and diabetes-like neuropathy than the wild-type ($PARP^{+/+}$) mice; *2*) to determine whether two structurally unrelated PARP inhibitors reverse established functional and metabolic changes of early PDN in diabetic rats; *3*) to localize the site(s) of PARP activation in the diabetic nerve; and *4*) to assess whether the presence of enhanced poly(ADP-ribosyl)ation correlates with the presence of neuropathic changes in the studied animal groups. The studies have been performed in streptozotocin (STZ)-induced diabetic and galactose models of PDN.

From the [1]Department of Internal Medicine, University of Michigan Medical Center, Ann Arbor, Michigan; [2]Veritas Laboratories Incorporation, Burlington, North Carolina; and [3]Inotek Pharmaceuticals Corporation, Beverly, Massachusetts.

Address correspondence and reprint requests to Dr. Irina G. Obrosova, Division of Endocrinology and Metabolism, Department of Internal Medicine, University of Michigan Medical Center, 1150 West Medical Center Dr., MSRB II, Room 5560, Ann Arbor, MI 48109-0678. E-mail: iobrosso@umich.edu.

Received for publication 5 August 2003 and accepted in revised form 20 November 2003.

P.P.'s current affiliation is with the National Institute on Alcohol Abuse and Alcoholism, Division of Intramural Clinical and Biological Research, Laboratory of Physiologic Studies, Section of Neuroendocrinology, Rockville, Maryland.

ABA, 3-aminobenzamide; AR, aldose reductase; Cr, creatine; DAB, diaminobenzidine; ISO, 1,5-isoquinolinediol; MAPK, mitogen-activated protein kinase; MNCV, motor nerve conduction velocity; NBF, nerve blood flow; PAR, poly(ADP-ribose); PARP, poly(ADP-ribose) polymerase; PCr, phosphocreatine; PDN, peripheral diabetic neuropathy; SNCV, sensory nerve conduction velocity; STZ, streptozotocin.

The galactose-fed rodents develop functional, metabolic, neurotrophic, and morphologic abnormalities similar to those observed in diabetes (31).

RESEARCH DESIGN AND METHODS

The experiments were performed in accordance with regulations specified by the National Institutes of Health "Principles of Laboratory Animal Care, 1985 Revised Version" and University of Michigan Protocol for Animal Studies.

Reagents. Unless otherwise stated, all chemicals were of reagent-grade quality and were purchased from Sigma Chemical (St. Louis, MO). Methanol (HPLC grade), perchloric acid, hydrochloric acid, and sodium hydroxide were obtained from Fisher Scientific (Pittsburgh, PA). Reagents for immunohistochemistry were purchased from Vector Laboratories (Burlingdale, CA) and Dako Laboratories (Santa Barbara, CA) as specified in the procedures.

Mouse study.

Model of STZ-induced diabetes. $PARP^{+/+}$ or $PARP^{-/-}$ mice (32), 129/SvxC57BL6 background, were treated with STZ (40 mg/kg; Upjohn, Kalamazoo, MI) intraperitoneally for 7 consecutive days. Blood samples for measurements of glucose were taken from the tail vein ~48 h after the last STZ injection and on days 17, 24, 31, 38, and 52. The mice with blood glucose ≥13.8 mmol/l were considered diabetic.

Model of galactose feeding. $PARP^{+/+}$ or $PARP^{-/-}$ mice were fed either standard mouse diet (PMI Nutrition Int., Brentwood, MO) or 30% mouse galactose diet (Test Diet, Richmond, IN). The duration of experiment was 52 days.

Rat study. Male Wistar rats (Charles River, Wilmington, MA), body weight 250–300 g, were fed a standard rat diet (PMI Nutrition Int.) and had access to water ad libitum. STZ-induced diabetes was induced as we described previously (4,12–14,29). Blood samples for measurements of glucose were taken from the tail vein ~48 h after the STZ injection and the day before the animals were killed. The rats with blood glucose ≥13.8 mmol/l were considered diabetic. The experimental groups comprised control and diabetic rats treated intraperitoneally with or without one of two PARP inhibitors, 3-aminobenzamide (ABA; 30 mg · kg body wt^{-1} · day^{-1}) and 1,5-isoquinolinediol (ISO; 3 mg · kg body wt^{-1} · day^{-1}). The treatments were started 2 weeks after the initial first 2 weeks without treatment. The duration of treatment was 2 weeks.

Anesthesia. We have previously reported (12,33) that a number of anesthetics distorts the profile of peripheral nerve metabolites, whereas a sedation by a short (~15–20 s) exposure to CO_2 with immediate cervical dislocation preserves high-energy phosphate levels in the range of those obtained after decapitation without any narcosis. For this reason, two different sets of animals were used for functional and metabolic studies. For functional studies that included measurements of MNCV and SNCV in the mice and measurements of nerve blood flow (NBF), MNCV, and SNCV in the rats, the mice were anesthetized by a mixture of ketamine and xylazine (75 and 5 mg/kg body wt, respectively, both intraperitoneally) and rats with inactin (65–85 mg/kg body wt, intraperitoneally). In the rat study, the onset (before induction of diabetes) MNCV and SNCV measurements were followed by the 2-week time point (beginning of interventions) and final (4-week time point) measurements. The latter were made before the assessment of NBF on the contralateral nerve. In all measurements, body temperature was monitored by a rectal probe and maintained at 37°C with a warming pad. Hind-limb skin temperature was also monitored by a thermistor and maintained between 36 and 38°C by radiant heat. For metabolic studies, the animals were sedated by CO_2 in a specially designed chamber (33) and immediately killed by cervical dislocation. The left nerves were rapidly dissected, blotted with fine filter paper to remove any accompanying blood, and frozen in liquid nitrogen for subsequent measurements of phosphocreatine (PCr) and creatine (Cr). The right nerves were fixed in 10% formalin and later used for immunohistochemistry.

Functional Studies.

Sciatic endoneurial nutritive NBF. NBF was assessed by microelectrode polarography and hydrogen clearance (34). The left carotid artery was cannulated with polyethylene tubing, and patency was maintained with heparinized saline (50 units/ml normal saline). The catheter was connected to a transducer, and the blood pressure was monitored by a MacLab data acquisition system. A tracheotomy was performed, and the animal was artificially respired with O_2:N_2 (20%:80%) using a small animal ventilator (Harvard Apparatus, South Natick, MA). The right sciatic nerve was exposed and gently dissected away from the surrounding tissue. The skin around the incision was positioned to create a reservoir. A ground electrode was inserted subcutaneously into the flank of the rat. Using a micromanipulator, a H_2-sensitive platinum electrode (tip diameter 1–2 μm; World Precision Instruments, Sarasota, FL) was inserted into the nerve above the trifurcation. Mineral oil maintained at 37°C was used to fill the reservoir and prevent diffusion of gases out of the nerve. The nerve was polarized with 0.25V, and when a stable baseline was achieved, the animal received a gas mixture containing 10% H_2, which was continued until the current change stabilized (10–30 min), at which time H_2 flow was terminated. Current recordings were made every 30 s until baseline levels were achieved (30–60 min). After the experiment, mono- or bi-exponential clearance curves were fitted to the data (Graphpad Software, La Jolla, CA). Nutritive NBF was taken as the slow component of the curve. An average of two determinations at different sites was used to determine nutritive NBF.

Sciatic MNCV. The left sciatic nerve was stimulated proximally at the sciatic notch and distally at the ankle via bipolar electrodes with supramaximal stimuli (8 V) at 20 Hz. The latencies of the compound muscle action potentials were recorded via bipolar electrodes from the first interosseous muscle of the hindpaw and measured from the stimulus artifact to the onset of the negative M-wave deflection. MNCV was calculated by subtracting the distal latency from the proximal latency, and the result was divided into the distance between the stimulating and recording electrode.

Digital SNCV. Hindlimb SNCV was recorded in the digital nerve to the second toe by stimulating with a square-wave pulse of 0.05-ms duration using the smallest intensity current that resulted in a maximal amplitude response. The sensory nerve action potential was recorded behind the medial malleolus. Sixteen responses were averaged to obtain the position of the negative peak. The maximal SNCV was calculated by measuring the latency to the onset/peak of the initial negative deflection and the distance between stimulating and recording electrodes.

Metabolic studies. The steady-state concentrations of PCr and Cr were assayed in perchloric acid extracts of femoral segments of the left sciatic nerve spectrofluorometrically by enzymatic procedures (4,13).

Immunohistochemical studies.

PAR immunoreactivity. All immunohistochemical samples were coded and examined by a single investigator in a blinded manner. Paraffin-embedded 5-μ thick longitudinal sections of sciatic nerve were deparaffinized in xylene and rehydrated in decreasing concentrations of ethanol followed by a 5-min incubation in PBS. Sections were treated with 0.3% hydrogen peroxide for 15 min to block endogenous peroxidase activity and then rinsed briefly in PBS. Nonspecific binding was blocked by incubating the slides for 1 h in 0.25% Triton/PBS containing 2% horse serum. To detect PAR, a routine histochemical procedure was applied as previously described (23) with minor modifications as follows. Mouse monoclonal anti-PAR antibody and isotype-matched control antibody were applied in a dilution of 1:400 for 1 h at room temperature. After extensive washing (three times, 10 min) with 0.25% Triton/PBS, immunoreactivity was detected with a biotinylated horse anti-mouse secondary antibody and the avidin-biotin-peroxidase complex, both supplied in the Vector Elite kit. Color was developed using the diaminobenzidine (DAB) substrate kit. Sections were then briefly rinsed in Tris/saline (pH 7.6) and incubated in Tris/Cobalt (pH 7.2) for 2 min. Sections were then counterstained with hematoxylin-eosin, dehydrated, and mounted in Permount. Microphotographs were taken with a Zeiss Axiolab microscope equipped with a Fuji HC-300C digital camera.

Double immunostaining. For localizing PAR in Schwann and endothelial cells, sciatic nerves were stained with *1*) anti-PAR antibody and anti–S-100 antibody and *2*) anti-PAR antibody and isolectin. S-100 is a Schwann cell marker (35), and isolectin (Griffonia simplifolia I-B4) is a plant protein that specifically binds to sugar residues on endothelial cells (36).

PAR and S-100 double immunostaining. Sciatic nerve segments were fixed overnight in 10% formalin, embedded in paraffin, and cut into 5-μm thick sections that were placed on Fisher MicroProbe slides to facilitate capillary action. Deparaffinized slides were placed in the Dako Antigen Retrieval solution, boiled for 20 min in a Black and Decker vegetable steamer, and rinsed in Dako Tris Buffer. From this point, two Vector staining kits were used. We used the Vector Stain Kit PK-6101 for S-100 staining performed in accordance with the manufacturer's instructions. First, the slides were blocked with normal goat serum and incubated for 20 min at 30°C. Then, they were incubated for 1 h at 30°C with anti–S-100 primary antibody applied in a dilution of 1:1,000 in Dako diluent, rinsed in Dako Tris buffer, incubated for 30 min at 30°C with a biotinylated anti-rabbit secondary antibody, and again rinsed in Dako Tris buffer. Then, the Vector Avidin-Biotin Complex (ABC) was applied, and the slides were incubated for 30 min at 30°C, rinsed in Dako Tris Buffer, and developed in Vector Red. After this step, the slides were rinsed in deionized water and stained for PAR. First, the slides were exposed to ice-cold trichloroacetic acid for 10 min and rinsed in deionized water and Dako Tris Buffer. Then, we used the Vector Stain Kit PK-6102 for PAR staining. The slides were blocked with normal horse serum and incubated for 20 min at 30°C. Then, they were incubated for 1 h at 30°C with anti-PAR primary antibody applied in a dilution of 1:300 in Dako diluent, rinsed in Dako Tris buffer, incubated for 30 min at 30°C with a biotinylated anti-mouse secondary antibody, and again rinsed in Dako Tris buffer. Then, the Vector ABC was

TABLE 1
Final body weights and blood glucose concentrations in experimental mice and rats

	Body weight (g)		Blood glucose (mmol/l)
	Initial*	Final	
Mouse			
STZ-induced diabetes model			
$PARP^{+/+}$	25.4 ± 0.7	27.8 ± 0.7	7.03 ± 0.43
$PARP^{+/+}$ diab	25.8 ± 0.5	24.5 ± 0.8§	22.7 ± 0.48†
$PARP^{-/-}$	24.0 ± 0.4	27.2 ± 0.8	5.72 ± 0.27
$PARP^{-/-}$ diab	25.4 ± 0.4	23.2 ± 0.9†	23.4 ± 0.86†
Galactose-fed model			
$PARP^{+/+}$	24.2 ± 0.6	25.6 ± 0.7	6.55 ± 0.15
$PARP^{+/+}$ gal	25.8 ± 0.8	25.1 ± 0.9	7.72 ± 0.12
$PARP^{-/-}$	23.8 ± 0.5	26.1 ± 0.5	6.45 ± 0.24
$PARP^{-/-}$ gal	26.0 ± 0.7	25.7 ± 0.7	6.43 ± 0.39
Rat			
Control	289 ± 4	462 ± 7	4.27 ± 0.17
Control + ABA	295 ± 4	416 ± 10§	4.22 ± 0.33
Control + ISO	286 ± 5	449 ± 11	3.88 ± 0.33
Diabetic	285 ± 4	390 ± 24†	20.4 ± 1.44†
Diabetic + ABA	279 ± 5	343 ± 9†‡	20.1 ± 0.50†
Diabetic + ISO	281 ± 3	363 ± 8†	20.8 ± 0.39†

*Data are means ± SE, n = 30–32. Before induction of STZ-induced diabetes; †significantly different from controls ($P < 0.01$, respectively); ‡significantly different from untreated diabetic group ($P < 0.01$). §Significantly different from controls ($P < 0.05$).

applied, and the slides were incubated for 30 min at 30°C, rinsed in Dako Tris Buffer, and developed in Vector DAB with nickel. The slides were rinsed in deionized water, counterstained with hematoxylin, dehydrated in ethanol, cleared in xylene, and coverslipped.

PAR and isolectin B4 double immunostaining. PAR staining has been performed as described above. Biotinylated isolectin was purchased from Vector Laboratories and used at 1:100 dilutions for 30 min at 30°C. Secondary antibody–horseradish peroxidase Avidin D was used at 1:1,000 dilutions for 30 min at 30°C. Isolectin staining was developed using the Vector DAB substrate with nickel.

Statistical analysis. The results are expressed as mean ± SE. Data were subjected to equality of variance F test and then to log transformation, if necessary, before one-way ANOVA. When overall significance ($P < 0.05$) was attained, individual between-group comparisons were made using the Student-Newman-Keuls multiple range test. Significance was defined at $P < 0.05$. When between-group variance differences could not be normalized by log transformation (datasets for body weights, plasma glucose, and some metabolic parameters), the data were analyzed by the nonparametric Kruskal-Wallis one-way ANOVA, followed by the Bonferroni/Dunn test for multiple comparisons.

RESULTS

The final body weights were comparably lower in diabetic $PARP^{+/+}$ and $PARP^{-/-}$ mice than in the corresponding control groups ($P < 0.01$; Table 1). Blood glucose concentrations were similarly elevated in diabetic $PARP^{+/+}$ and $PARP^{-/-}$ mice compared with the corresponding control groups at all time points (Fig. 1).

The final body weights were similar in control $PARP^{+/+}$, control $PARP^{-/-}$, galactose-fed $PARP^{+/+}$, and galactose-fed $PARP^{-/-}$ mice. The final blood glucose concentrations were also similar among the groups.

The final body weights were lower in diabetic rats compared with controls ($P < 0.01$). They were slightly but significantly lower in the ABA-treated control and diabetic rats compared with the corresponding untreated groups

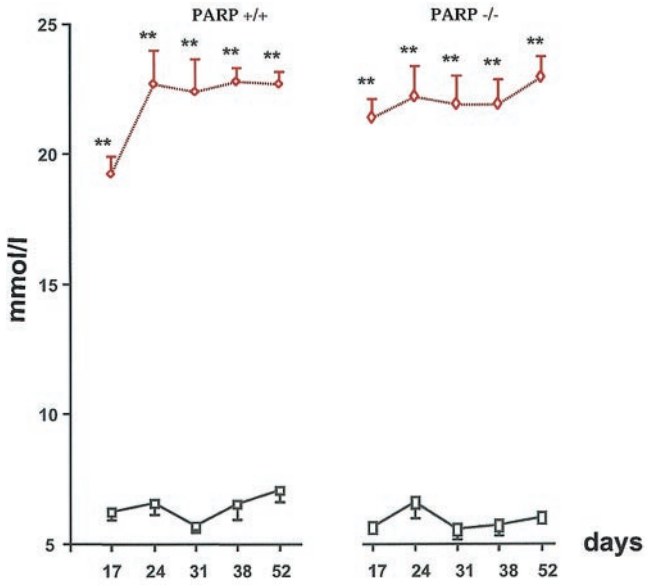

FIG. 1. Blood glucose concentrations in control (solid black line) and diabetic (dashed red line) $PARP^{+/+}$ and $PARP^{-/-}$ mice (mean ± SE, n = 6–10). **$P < 0.01$ vs. corresponding nondiabetic groups. The time points reflect days after the last STZ injection.

($P < 0.05$ and $P < 0.01$, respectively). ISO treatment did not affect body weights in either control or diabetic rats. Blood glucose concentrations were increased ~fivefold in diabetic rats compared with controls ($P < 0.01$). Neither ABA nor ISO affected blood glucose concentrations in either control or diabetic rats.

$PARP^{+/+}$ and $PARP^{-/-}$ mice seemed remarkable different in susceptibility to early diabetic and galactose-induced neuropathy. Diabetic $PARP^{+/+}$ mice developed motor and sensory nerve conduction deficits in 17 days after induction of diabetes (Fig. 2*A*) that persisted at all time points studied. In contrast, diabetic $PARP^{-/-}$ mice preserved normal MNCV and SNCV throughout the experiment (Fig. 2*B*). A similar phenomenon has been observed in the galactose model. The galactose-fed $PARP^{+/+}$ mice progressively developed MNCV and SNCV deficits (Fig. 2*A*). Both MNCV and SNCV values achieved significant differences from the corresponding control groups 31 days after the beginning of galactose feeding, and the deficits in both variables progressed with the duration of experiment. The galactose-fed $PARP^{-/-}$ mice were resistant to both motor and sensory nerve conduction slowing and had MNCV and SNCV values indistinguishable from those in the mice that were fed normal diet at all time points (Fig. 2*B*).

The onset MNCV and SNCV (before induction of STZ-induced diabetes) for all experimental groups in the rat study, as well as MNCV and SNCV at the beginning of interventions, i.e., the 2-week time point, are given in Table 2. Final MNCV and SNCV (Fig. 3*A* and *B*) were 25 and 23% reduced in diabetic rats compared with controls, respectively. MNCV deficit was 93 and 97% corrected by ISO and ABA, respectively, whereas SNCV deficit was 89 and 92% corrected. Neither ABA nor ISO had any effect on either MNCV or SNCV in nondiabetic rats.

Diabetes-induced 49% reduction in sciatic endoneurial nutritive NBF was 84 and 92% reversed by ISO and ABA,

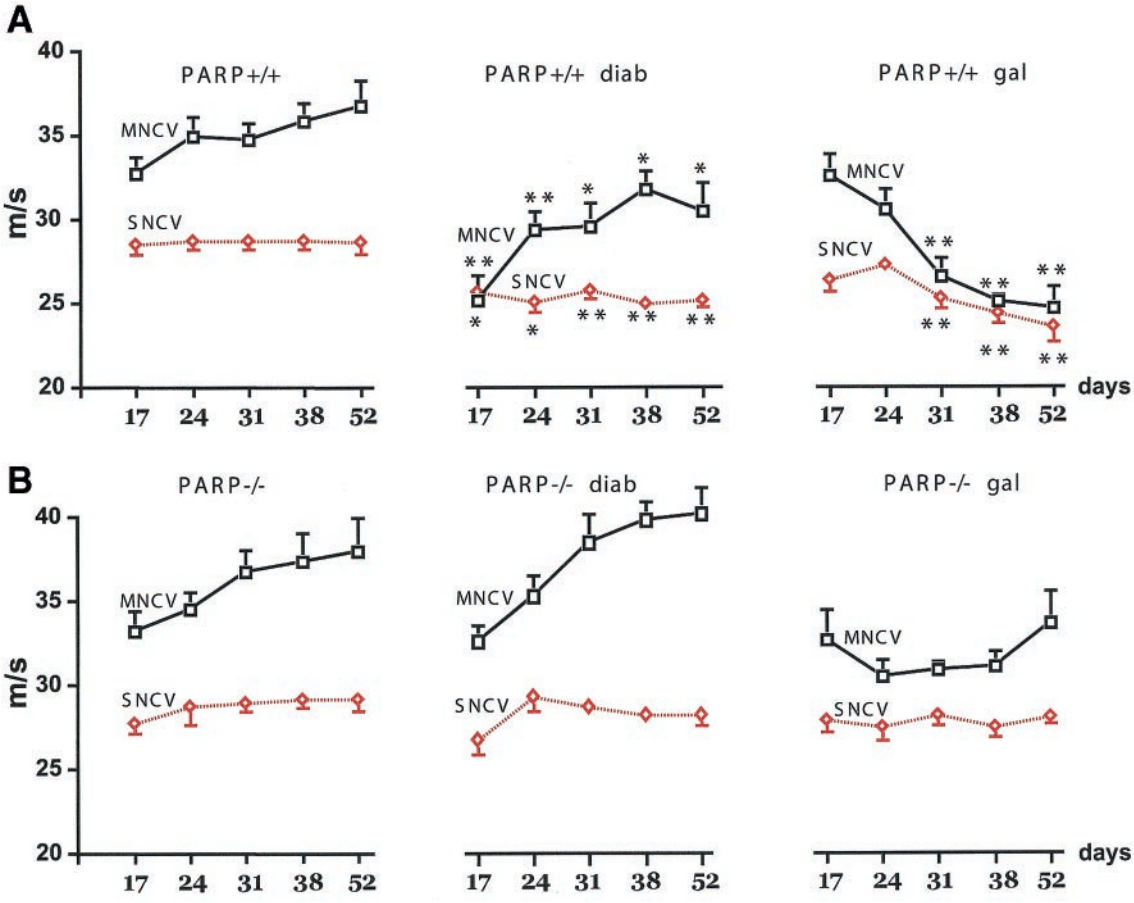

FIG. 2. MNCV and SNCV in control, diabetic, and galactose-fed PARP$^{+/+}$ (*A*) and PARP$^{-/-}$ (*B*) mice (mean ± SE, n = 6–10). *P < 0.05 and **P < 0.01 vs. nondiabetic, nongalactosemic PARP$^{+/+}$ mice. The time points for diabetic groups reflect days after the last STZ injection.

respectively (Fig. 3*C*). Diabetes-associated 20% decrease in mean systemic blood pressure (Fig. 3*D*) was corrected by both PARP inhibitors to the levels that were not significantly different from either control or diabetic rats. Diabetes-induced 37% deficit in endoneurial vascular conductance (Fig. 3*E*), i.e., NBF normalized for blood pressure, was 92 and 98% reversed by ISO and ABA, respectively.

Sciatic nerve PCr concentration and PCr/Cr ratio were reduced in both diabetic and galactose-fed PARP$^{+/+}$ mice compared with the corresponding controls (Table 3). In contrast, both diabetic and galactose-fed PARP$^{-/-}$ mice preserved normal nerve PCr concentration and PCr/Cr ratio. Nerve Cr concentrations were similar among the groups. In the rat study, PCr concentration and PCr/Cr ratio but not Cr concentration were decreased in diabetic rats compared with controls. PARP inhibitors did not affect PCr and Cr concentrations and PCr/Cr ratio in controls rats. ABA restored normal PCr concentration and PCr/Cr ratio in diabetic rats. With ISO treatment, PCr concentration was normalized, whereas PCr/Cr ratio showed a trend toward normalization, but the difference with the untreated diabetic group did not achieve statistical significance.

TABLE 2
The onset* and 2-week MNCV and SNCV in rat experimental groups

	MNCV (m/s)		SNCV (m/s)	
	Onset	2 Weeks	Onset	2 Weeks
Control	55.4 ± 0.7	56.6 ± 1.3	36.5 ± 0.4	37.1 ± 0.5
Control + ABA	55.6 ± 0.7	57.3 ± 1.1	36.5 ± 0.5	37.2 ± 0.4
Control + ISO	56.9 ± 1.8	57.2 ± 1.2	36.7 ± 0.6	36.9 ± 0.4
Diabetic	55.4 ± 0.7	45.8 ± 1.1†	37.1 ± 0.4	32.0 ± 0.7†
Diabetic + ABA	56.2 ± 1.2	44.8 ± 0.8†	36.8 ± 0.5	31.4 ± 0.4†
Diabetic + ISO	56.5 ± 1.6	45.3 ± 1.3†	36.9 ± 0.4	31.9 ± 0.7†

*Data are mean ± SE, n = 6–10. Before induction of STZ-induced diabetes; †significantly different from the corresponding onset values (P < 0.01).

PAR-reactive nuclei were localized in both endothelial (Fig. 4*D*) and Schwann (Fig. 4*F*) cells of diabetic peripheral nerve. Increased sciatic nerve PAR immunoreactivity was found in all experimental groups with manifest diabetic or diabetes-like neuropathy (Fig. 5*A*, 4, and *B*, 2 and 6). In contrast, PAR staining was barely detectable in any of the groups with normal functional and energetic state of the peripheral nerve (Fig. 5*A*, 1,2,3,5,6 and *B*, 1,3,4,5).

DISCUSSION

Studies with the "universal" antioxidant, DL-α-lipoic acid (12,16,18), other antioxidants and metal chelators (14–

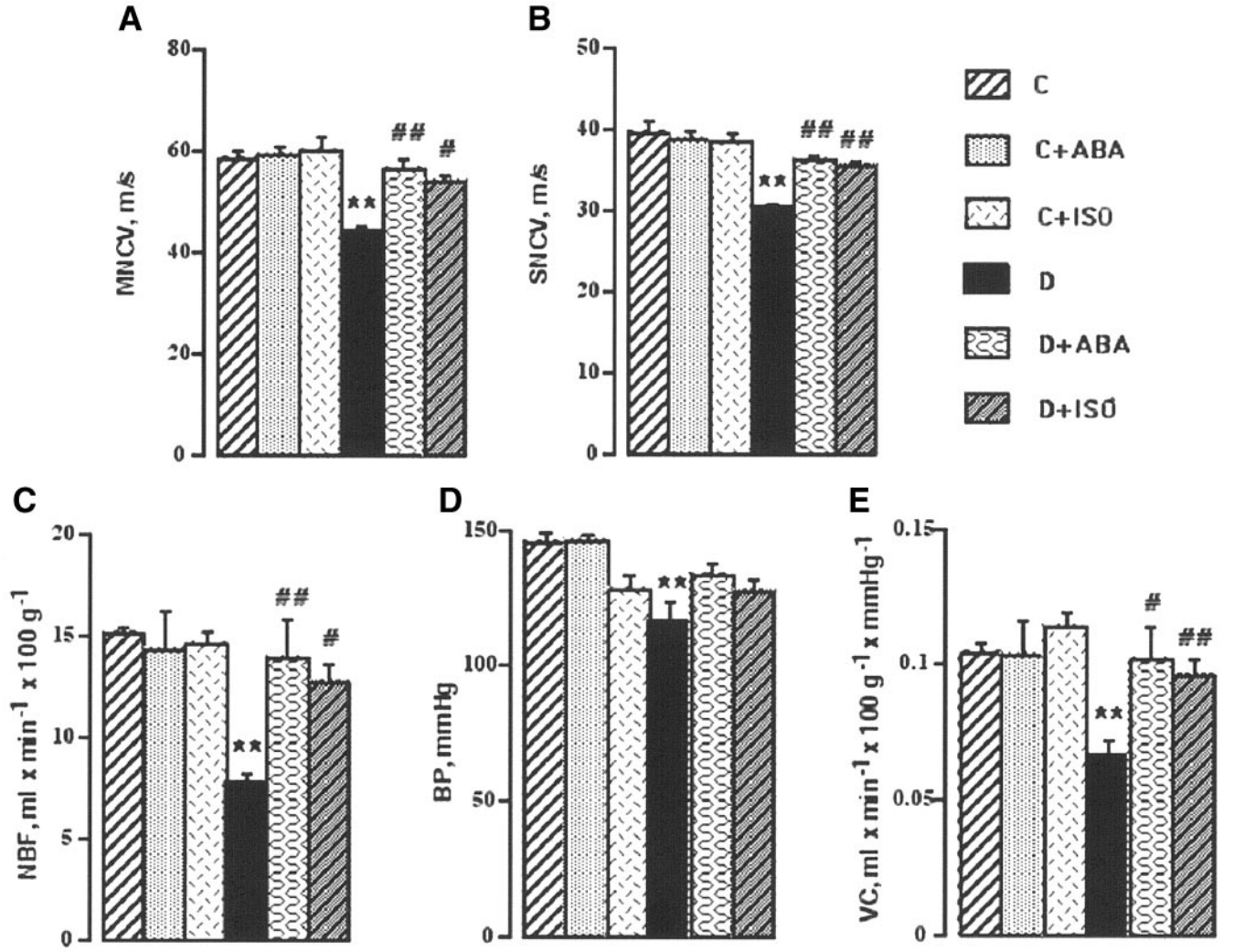

FIG. 3. Final MNCV (*A*), SNCV (*B*), NBF (*C*), blood pressure (*D*), and vascular conductance (*E*) in control (C) and diabetic (D) rats treated with or without ABA or ISO (mean ± SE, $n = 6–10$). $^{**}P < 0.01$ vs. control group and $^{\#}P < 0.05$ and $^{\#\#}P < 0.01$ vs. untreated diabetic group.

16,20), and pro-oxidants (18,19) support the central role for oxidative stress in NBF and conduction deficits, metabolic changes, impaired neurotropism, and morphologic abnormalities characteristic for PDN. Oxidative injury is manifested by *1*) accumulation of lipid peroxidation products; depletion of GSH, ascorbate, and taurine; changes in the glutathione and ascorbate redox states; downregulation of superoxide dismutase; and catalase activities in the peripheral nerve (4,5,8,12–15); *2*) increased production of superoxide and nitrotyrosine (a marker of peroxynitrite-induced injury) in *vasa nervorum* (16,17); and *3*) elevated concentrations of 8-hydroxy-2′-deoxyguanosine (a marker of DNA oxidative damage) in dorsal root ganglion of STZ-induced diabetic rats (30). Reactive oxygen species affect multiple signal transduction and metabolic pathways. One of the important features of free radical and oxidant-initiated metabolic response is PARP activation (22–25). PARP activation has an important role in cardiovascular and neurodegenerative diseases and inflammation (22–24,28). Growing evidence suggests an important role of PARP activation in the pathogenesis of type 1 (insulin-dependent) diabetes and diabetic complications (24). PARP activation manifested by PAR accumulation is present in vascular endothelium (22,23), retina (37), and renal cortex (29) of STZ-induced diabetic rats and mice and skin vessels of diabetic patients (38). The present study generated the first evidence of *1*) enhanced poly-(ADP-ribosyl)ation in the rat and mouse diabetic peripheral nerve and *2*) the key role of PARP activation in functional and metabolic changes characteristic for the early stage of PDN.

Our findings in both rat and mouse models suggest that PARP activation is required for development of both motor and sensory neuropathy. Diabetic PARP-deficient mice are protected from both MNCV and SNCV deficits that were clearly manifest in diabetic $PARP^{+/+}$ mice. Galactose-fed $PARP^{+/+}$ mice had a pattern of MNCV and SNCV slowing different from diabetic $PARP^{+/+}$ mice, i.e., 30% galactose-induced changes developed later and were more severe than those observed in diabetic animals. It should be pointed out that there was a slight (nonsignificant) decline of MNCV in galactose-fed $PARP^{-/-}$ mice, which suggests that further, long-term studies are needed to sort out whether PARP absence or PARP inhibition is protective against advanced galactose-induced neuropathy. Two structurally different PARP inhibitors, ABA and

TABLE 3
Nerve energy state in the mouse and rat models

	PCr (μmol/g)	PCr/Cr
Mouse		
STZ-induced diabetes model		
$PARP^{+/+}$	0.852 ± 0.057	0.161 ± 0.012
$PARP^{+/+}$ diab	0.347 ± 0.037†	0.063 ± 0.013†
$PARP^{-/-}$	0.832 ± 0.092	0.140 ± 0.013
$PARP^{-/-}$ diab	0.873 ± 0.097	0.153 ± 0.027
Study in galactose-fed model		
$PARP^{+/+}$	0.869 ± 0.032	0.206 ± 0.023
$PARP^{+/+}$ gal	0.481 ± 0.082*	0.105 ± 0.006*
$PARP^{-/-}$	0.829 ± 0.094	0.209 ± 0.023
$PARP^{-/-}$ gal	0.753 ± 0.137	0.185 ± 0.029
Rat		
Control	3.45 ± 0.22	0.898 ± 0.053
Control + ABA	3.03 ± 0.25	0.755 ± 0.033
Control + ISO	3.34 ± 0.18	0.725 ± 0.057
Diabetic	2.36 ± 0.14†	0.553 ± 0.043†
Diabetic + ABA	3.30 ± 0.18‡	0.697 ± 0.030*
Diabetic + ISO	3.48 ± 0.10§	0.786 ± 0.012‡

Data are means ± SE, $n = 6–8$. *$P < 0.05$ and †$P < 0.01$ compared with controls; ‡$P < 0.05$ and §$P < 0.01$ compared with the untreated diabetic group.

ISO, reversed established MNCV and SNCV deficits in STZ-induced diabetic rats. This effect was not due to restoration of normoglycemia or alleviation of hyperglycemia, which takes place when PARP inhibitor treatment is started before or shortly after STZ injection (24). Final blood glucose concentrations were similarly, ~fivefold, higher in untreated diabetic rats and diabetic rats that were treated with ABA or ISO compared with the nondiabetic control group. Findings from our laboratory (39) (Table 2, Fig. 3 in the present study) and a recent preliminary report (40) suggest that *1*) the difference in final nerve conduction velocities between control and diabetic animals results from two independent processes: diabetes-associated actual nerve conduction slowing and diabetes-induced retardation of normal nerve growth and maturation; and *2*) PARP inhibitor treatment acts on both components with predominant effect on diabetes-induced slowing of nerve conduction.

The fundamental role of PARP in the pathogenesis of diabetic neuropathy is consistent with importance of enhanced poly(ADP-ribosyl)ation in oxidative stress-induced energy failure. From a variety of metabolic parameters, nerve energy state correlates best with nerve conduction (4,12,13) because nerve plasma membrane potential is maintained by energy-dependent processes, i.e., depends on cytosolic ATP/ADP ratio. ATP concentrations are not depleted in the peripheral nerve in, at least, short-term diabetes, and it is another high-energy phosphate compound, PCr, that responds to diabetic condition (4,12,13). The decrease in PCr/Cr ratio (an index of free cytosolic ATP/ADP ratio) accounts for chronic depolarization and Na^+ channel inactivation with resulting reduced excitability and nerve conduction deficit in diabetic nerves. The decrease in nerve PCr concentration and PCr/Cr ratio was observed in both galactose-fed and diabetic $PARP^{+/+}$ mice compared with the corresponding controls. In contrast, both galactose-fed and diabetic $PARP^{-/-}$ mice preserved normal PCr concentration and PCr/Cr ratio. These findings are in line with the role of PARP activation in depleting energy stores and, in particular, PCr concentrations under conditions of enhanced oxidative stress.

PARP activation can contribute to energy deficiency in the diabetic nerve via both vascular and nonvascular mechanisms. PARP inhibition caused correction of diabetes-associated endoneurial nutritive NBF and vascular conductance deficits in the peripheral nerve. This is consistent with a key role for PARP activation in endothelial dysfunction (22,23) as well as a reversal of endothelium-dependent vasodilation with short-term PARP inhibitor treatment (41). Several groups have reported findings suggesting a causal relation between peripheral nerve perfusion and conduction deficits (2,4,8,13,15,16). Both NBF and conduction deficits are corrected by a number of pharmacologic agents, e.g., AR inhibitors (2,4), aminoguanidine (42), antioxidants (16,42). However, this "parallelism" should be interpreted with caution. Both AR inhibitors and antioxidants exert favorable metabolic effects that are independent from the state of perfusion and oxygen supply. For example, both classes of the compounds counteract diabetes-induced inhibition of glycolysis, NAD^+/NADH redox imbalances, and energy failure in such nonvascular tissue as ocular lens (43,44). The role for nonvascular AR in diabetes-associated MNCV deficit is clearly illustrated by the finding of a significantly greater reduction in MNCV in both diabetic and galactosemic transgenic mice overexpressing AR specifically in the Schwann cells of peripheral nerve under the control of the rat myelin protein zero (P_0) promoter compared with the corresponding nontransgenic mice with normal AR content (5). A number of other studies support the role for nonvascular mechanisms in diabetes-associated peripheral nerve dysfunction. Administration of the neurotrophic factor prosaposin to rats with PDN or galactose-induced neuropathy prevented nerve conduction slowing, without counteracting a decrease in NBF (31). Treatment of diabetic rats with a sonic hedgehog-IgG fusion protein *1*) ameliorated retrograde transport of nerve growth factor and sciatic nerve concentrations of calcitonin gene–related product and neuropeptide Y, *2*) restored normal MNCV and SNCV, and *3*) maintained the axonal caliber of large myelinated fibers, in the absence of any improvement in NBF (45). Furthermore, our recent study (46) revealed that treatment with the orally active PARP inhibitor PJ34 resulted in essential normalization of both MNCV and SNCV deficits and nerve energy state but only a modest (17%) improvement of NBF in STZ-induced diabetic rats. Thus, there is an important nonvascular component in the PARP action. PARP activation has been recently revealed to be responsible for diabetes-associated decrease of glyceraldehyde 3-phosphate dehydrogenase activity and inhibition of glycolysis (47). Conversely, PARP inhibition should activate glucose utilization by the glycolytic pathway. Beneficial effects of PARP inhibition (restoration of normal nicotinamide adenine nucleotide content and energy state) have been reported for high glucose–exposed endothelium (22). Similar metabolic changes, with resulting improvement of nerve function, probably

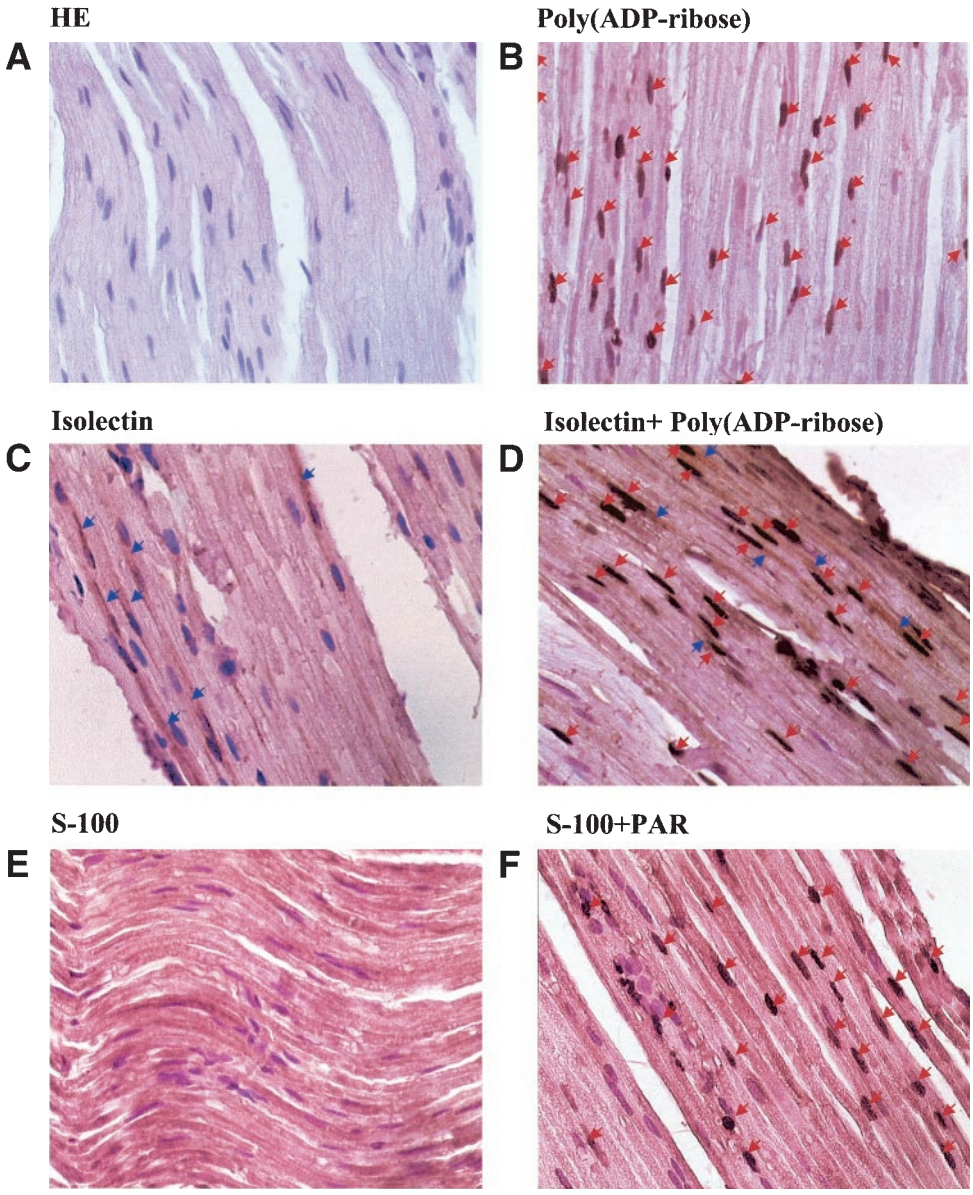

FIG. 4. Representative microphotographs of the sciatic nerves of diabetic rats. *A*: Staining with hematoxylin-eosin, peripheral nerve histology control. *B*: Staining with anti-PAR antibody; red arrows indicate nuclear PAR staining. *C*: Staining with isolectin; blue arrows indicate isolectin-labeled endothelium. *D*: PAR-containing nuclei (red arrows) localized inside isolectin-labeled brown endothelium (blue arrows). *E*: Anti–S-100 antibody-labeled Schwann cells. *F*: PAR-containing nuclei (red arrows) localized inside anti–S-100 antibody-labeled Schwann cells. Magnification ×400.

occur in nerve Schwann cells that clearly display enhanced poly(ADP-ribosyl)ation under diabetic conditions.

PARP activation can contribute to PDN via a number of other mechanisms. Those include activation of protein kinase C and mitogen-activated protein kinases (MAPKs), as well as nonenzymatic glycation, all of which occur as a result of diversion of the glycolytic flux toward the formation of diacylglycerol and methylglyoxal under conditions of PARP-mediated inhibition of glyceraldehyde 3-phosphate dehydrogenase (47). The role for protein kinase C activation in PDN has been established with structurally diverse protein kinase C inhibitors (2,8). MAPKs, e.g., ERK, p38 MAPK, JNK, play an important role in the breakdown of neuronal phenotype (19) and aberrant neurofilament phosphorylation, a phenomenon involved in the etiology of diabetic sensory polyneuropathy (48). Sural nerve JNK activation and increases in total levels of p38 and JNK have been detected in patients with both type 1 and type 2 diabetes. The role for methylglyoxal in advanced glycation end product formation is well established (7). Advanced glycation end products, in turn, exacerbate oxidative stress during interaction with their receptors (10), thus creating a "vicious cycle" and contributing to the pathogenesis of PDN via several mechanisms (6,7).

An alternative way in which PARP may influence the development of PDN involves regulation of transcription factors and associated gene expression (27,28). PARP-1 has been reported either to activate or repress transcription activity. PARP-1 effects on transcription activity may involve direct protein-protein interaction with PARP-1 or the catalytic activity of the PARP-1 enzyme, which can

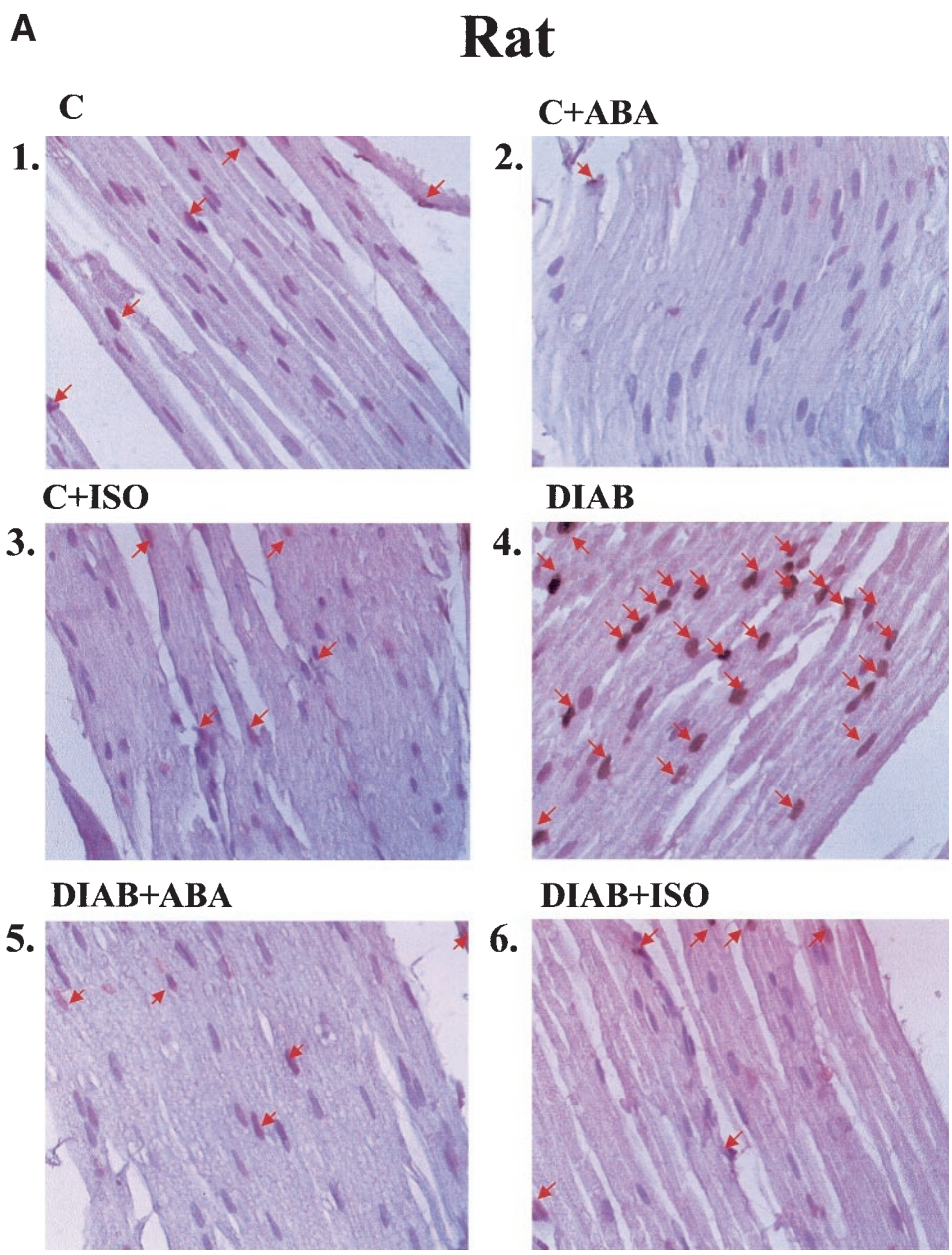

FIG. 5. Representative microphotographs of nuclear PAR immunostaining (red arrows) in the rat (*A*) and mouse (*B*) sciatic nerves. Magnification ×400.

poly(ADP-ribosyl)ate transcription factors. Transcription factors such as AP-2, B-MYP, Oct-1, YY-1, and TEF-1 bind directly to PARP-1; others such as p53, fos, and RNA polymerases I and II are poly(ADP-ribosyl)ated. PARP-1 participates in the activation of nuclear factor-κB independent of energy depletion by binding directly to nuclear factor-κB or poly(ADP-ribosyl)ating nuclear factor-κB. In addition, PARP-1 regulates other important transcription factors, such as AP-1, SP-1, YY-1, and Stat-1, that, in turn, control the expression of a variety of genes, including interleukin-6, pro-interleukin-1β, intracellular adhesion molecule-1, tumor necrosis factor-α, endothelin-1, cyclooxygenase-2, and inducible nitric oxide synthase. Expression of all of those genes seemed to be PARP dependent (28,29). Endothelin-1 (49), cyclooxygenase-2 (50), and, potentially, inflammatory mechanisms and inducible nitric oxide synthase participate in the pathogenesis of PDN.

In conclusion, our findings indicate the important role of PARP in diabetic motor and sensory nerve conduction deficits, neurovascular dysfunction, and energy failure characteristic for PDN. The lack of any difference in either MNCV or SNCV between nondiabetic, nongalactosemic wild-type, and PARP-deficient mice and the presence of PARP activation and energy failure in all experimental groups that manifest diabetic or diabetes-like neuropathy in both rat and mouse studies point to the importance of the catalytic activation rather than the physical presence of PARP for the development of functional and metabolic changes in the diabetic nerve. PARP activation triggers multiple mechanisms initiated by oxidative stress. The findings suggest that PARP inhibition can provide a novel approach for prevention and treatment of PDN and related diabetic complications, although additional studies with

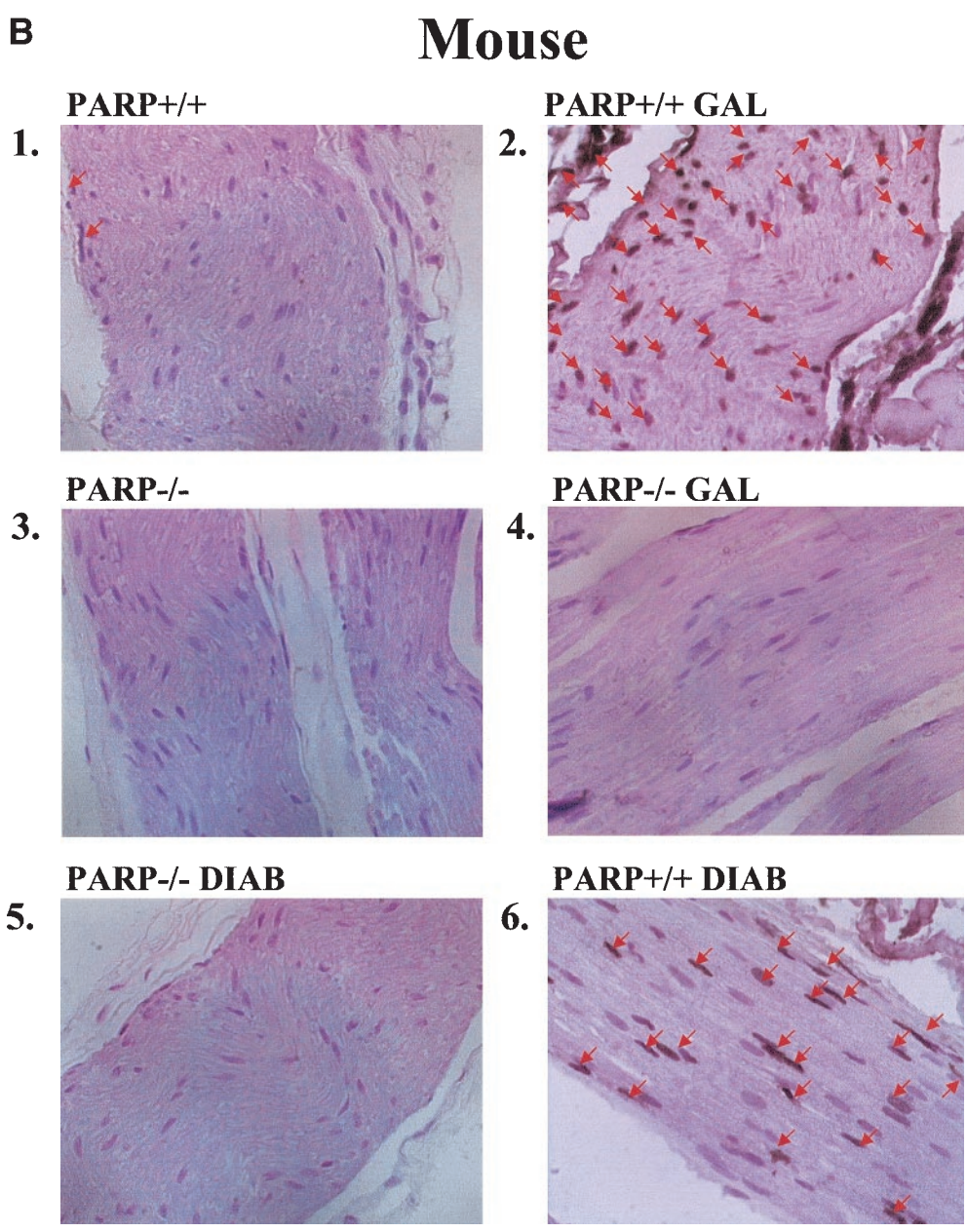

FIG. 5—*Continued*.

other end points and in the chronic model are needed to verify whether it is really the case.

ACKNOWLEDGMENTS

The study was supported by the American Diabetes Association Research Grant and the National Institutes of Health Grant DK59809-01 (both to I.G.O.), the Juvenile Diabetes Research Foundation Center for the Study of Complications of Diabetes Grant 4-200-421 (I.G.O., M.J.S.), and the National Institutes of Health Grant HL/DK 71215-01 (C.S.).

We are grateful to A.P. Mizisin, University of California-San Diego, CA, for valuable recommendations regarding immunohistochemical colocalization studies. P. Pacher and K. Komjáti are on leave of absence from the Department of Pharmacology and Institute of Human Physiology and Clinical Experimental Research, Semmelweis University, Budapest, Hungary.

REFERENCES

1. Boulton AJ: Treatments for diabetic neuropathy. *Curr Diab Rep* 1:127–132, 2001
2. Nakamura J, Kato K, Hamada Y, Nakayama M, Chaya S, Nakashima E, Naruse K, Kasuya Y, Mizubayashi R, Miwa K, Yasuda Y, Kamiya H, Ienaga K, Sakakibara F, Koh N, Hotta N: A protein kinase C-β-selective inhibitor ameliorates neural dysfunction in streptozotocin-induced diabetic rats. *Diabetes* 48:2090–2095, 1998
3. Yagihashi S, Yamagishi SI, Wada R, Baba M, Hohman TC, Yabe-Nishimura C, Kokai Y: Neuropathy in diabetic mice overexpressing human aldose reductase and effects of aldose reductase inhibitors. *Brain* 124:2448–2458, 2001
4. Obrosova IG, Van Huysen C, Fathallah L, Cao XC, Greene DA, Stevens MJ: An aldose reductase inhibitor reverses early diabetes-induced changes in peripheral nerve function, metabolism, and antioxidative defense. *FASEB J* 16:123–125, 2002
5. Song Z, Fu DTW, Chan Y-S, Leung S, Chung SSM, Chung SK: Transgenic mice overexpressing aldose reductase in Schwann cells show more severe nerve conduction velocity deficit and oxidative stress under hyperglycemic stress. *Mol Cell Neurosci* 23 :638–647, 2003
6. Dickinson PJ, Carrington AL, Frost GS, Boulton AJ: Neurovascular dis-

ease, antioxidants and glycation in diabetes. *Diabetes Metab Res Rev* 18:260–272, 2002
7. Thornalley PJ: Glycation in diabetic neuropathy: characteristics, consequences, causes, and therapeutic options. *Int Rev Neurobiol* 50:37–57, 2002
8. Cameron NE, Cotter MA, Jack AM, Basso MD, Hohman TC: Protein kinase C effects on nerve function, perfusion, Na(+), K(+)-ATPase activity and glutathione content in diabetic rats. *Diabetologia* 42:1120–1130, 1999
9. El-Remessy AB, Abou-Mohamed G, Caldwell RW, Caldwell RB: High glucose-induced tyrosine nitration in endothelial cells: role of eNOS uncoupling and aldose reductase activation. *Invest Ophthalmol Vis Sci* 44:3135–3143, 2003
10. Stern DM, Yan SD, Yan SF, Schmidt AM: Receptor for advanced glycation endproducts (RAGE) and the complications of diabetes. *Ageing Res Rev* 1:1–15, 2002
11. Abiko T, Abiko A, Clermont AC, Shoelson B, Horio N, Takahashi J, Adamis AP, King GL, Bursell SE: Characterization of retinal leukostasis and hemodynamics in insulin resistance and diabetes: role of oxidants and protein kinase C activation. *Diabetes* 52:829–837, 2003
12. Stevens MJ, Obrosova I, Cao X, Van Huysen C, Greene DA: Effects of DL-α-lipoic acid on peripheral nerve conduction, blood flow, energy metabolism, and oxidative stress in experimental diabetic neuropathy. *Diabetes* 49:1006–1105, 2000
13. Obrosova IG, Van Huysen C, Fathallah L, Cao X, Stevens MJ, Greene DA: Evaluation of alpha(1)-adrenoceptor antagonist on diabetes-induced changes in peripheral nerve function, metabolism, and antioxidative defense. *FASEB J* 14:1548–1558, 2000
14. Obrosova IG, Fathallah L, Stevens MJ: Taurine counteracts oxidative stress and nerve growth factor deficit in early experimental diabetic neuropathy. *Exp Neurol* 172:211–219, 2001
15. Low PA, Nickander KK, Tritschler HJ: The roles of oxidative stress and antioxidant treatment in experimental diabetic neuropathy. *Diabetes* 46 (Suppl. 2):S38–S42, 1997
16. Coppey LJ, Gellett JS, Davidson EP, Dunlap JA, Lund DD, Yorek MA: Effect of antioxidant treatment of streptozotocin-induced diabetic rats on endoneurial blood flow, motor nerve conduction velocity, and vascular reactivity of epineurial arterioles of the sciatic nerve. *Diabetes* 50:1927–1937, 2001
17. Coppey LJ, Gellett JS, Davidson EP, Yorek MA: Preventing superoxide formation in epineurial arterioles of the sciatic nerve from diabetic rats restores endothelium-dependent vasodilation. *Free Radic Res* 37:33–40, 2003
18. Hounsom L, Corder R, Patel J, Tomlinson DR: Oxidative stress participates in the breakdown of neuronal phenotype in experimental diabetic neuropathy. *Diabetologia* 44:424–428, 2001
19. Purves T, Middlemas A, Agthong S, Jude EB, Boulton AJ, Fernyhough P, Tomlinson DR: A role for mitogen-activated protein kinases in the etiology of diabetic neuropathy. *FASEB J* 15:2508–2514, 2001
20. Sagara M, Satoh J, Wada R, Yagihashi S, Takahashi K, Fukuzawa M, Muto G, Muto Y, Toyota T: Inhibition of development of peripheral neuropathy in streptozotocin-induced diabetic rats with N-acetylcysteine. *Diabetologia* 39:263–269, 1996
21. Hoeldtke RD, Bryner KD, McNeill DR, Hobbs GR, Riggs JE, Warehime SS, Christie I, Ganser G, Van Dyke K: Nitrosative stress, uric acid, and peripheral nerve function in early type 1 diabetes. *Diabetes* 51:2817–2825, 2002
22. Garcia Soriano F, Virag L, Jagtap P, Szabo E, Mabley JG, Liaudet L, Marton A, Hoyt DG, Murthy KG, Salzman AL, Southan GJ, Szabo C: Diabetic endothelial dysfunction: the role of poly (ADP-ribose) polymerase activation. *Nat Med* 7:108–113, 2001
23. Pacher P, Liaudet L, Soriano FG, Mabley JG, Szabo E, Szabo C: The role of poly (ADP-ribose) polymerase activation in the development of myocardial and endothelial dysfunction in diabetes. *Diabetes* 51:514–521, 2002
24. Virag L, Szabo C: The therapeutic potential of poly(ADP-ribose) polymerase inhibitors. *Pharmacol Rev* 54:375–429, 2002
25. Yu SW, Wang H, Poitras MF, Coombs C, Bowers WJ, Federoff HJ, Poirier GG, Dawson TM, Dawson VL: Mediation of poly (ADP-ribose) polymerase-1-dependent cell death by apoptosis-inducing factor. *Science* 297:259–263, 2002
26. Berciano MT, Fernandez R, Pena E, Calle E, Villagra NT, Lafarga M: Necrosis of Schwann cells during tellurium-induced primary demyelination: DNA fragmentation, reorganization of splicing machinery, and formation of intranuclear rods of actin. *J Neuropathol Exp Neurol* 58:1234–1243, 1999
27. Soldatenkov VA, Chasovskikh S, Potaman VN, Trofimova I, Smulson ME, Dritschilo A: Transcriptional repression by binding of poly (ADP-ribose) polymerase to promoter sequences. *J Biol Chem* 277:665–670, 2002
28. Ha HC, Hester LD, Snyder SH: Poly(ADP-ribose) polymerase-1 dependence of stress-induced transcription factors and associated gene expression in glia. *Proc Natl Acad Sci U S A* 99:3270–3275, 2002
29. Minchenko AG, Stevens MJ, White L, Abatan OI, Komjati K, Pacher P, Szabo C, Obrosova IG: Diabetes-induced overexpression of endothelin-1 and endothelin receptors in the rat renal cortex is mediated via poly (ADP-ribose) polymerase activation. *FASEB J* 17:1514–1516, 2003
30. Schmeichel AM, Schmelzer JD, Low PA: Oxidative injury and apoptosis of dorsal root ganglion neurons in chronic experimental diabetic neuropathy. *Diabetes* 52:165–171, 2003
31. Mizisin AP, Steinhardt RC, O'Brien JS, Calcutt NA: TX14(A), a prosaposin-derived peptide, reverses established nerve disorders in streptozotocin-diabetic rats and prevents them in galactose-fed rats. *J Neuropathol Exp Neurol* 60:953–960, 2001
32. Wang ZQ, Auer B, Stingl L, Berghammer H, Haidacher D, Schweiger M, Wagner EF: Mice lacking ADPRT and poly (ADP-ribosyl) ation develop normally but are susceptible to skin disease. *Genes Dev* 9:509–520, 1995
33. Obrosova IG, Fathallah L, Lang HJ, Greene DA: Evaluation of a sorbitol dehydrogenase inhibitor on diabetic peripheral nerve metabolism: a prevention study. *Diabetologia* 42:1187–1194, 1999
34. Tuck RR, Schmelzer JD, Low PA: Endoneurial blood flow and oxygen tension in the sciatic nerves of rats with experimental diabetic neuropathy. *Brain* 107:935–950, 1984
35. Symons NA, Danielsen N, Harvey AR: Migration of cells into and out of peripheral nerve isografts in the peripheral and central nervous systems of the adult mouse. *Eur J Neurosci* 14:522–532, 2001
36. Nasu K, Whyte A, Green SJ, Evans PC, Kilshaw PJ: Alpha-galactosyl-mediated activation of porcine endothelial cells: studies on CD31 and VE-cadherin in adhesion and signaling. *Transplantation* 68:861–867, 1999
37. Obrosova I, Seigel G, Frank R, Abatan O, Pacher P, Komjati K, Stevens M, Szabo C: Early diabetes-induced changes in the retina: comparison of STZ-induced models in rat and mouse (Abstract). *Diabetes* 52 (Suppl. 1):A202, 2003
38. Szabo C, Zanchi A, Komjati K, Pacher P, Krolewski AS, Quist WC, LoGerfo FW, Horton ES, Veves A: Poly (ADP-ribose) polymerase is activated in subjects at risk of developing type 2 diabetes and is associated with impaired vascular reactivity. *Circulation* 106:2680–2686, 2002
39. Stevens MJ, Lattimer SA, Feldman EL, Helton ED, Millington DS, Sima AA, Greene DA: Acetyl-L-carnitine deficiency as a cause of altered nerve myo-inositol content, Na, K-ATPase activity, and motor conduction velocity in the streptozotocin-diabetic rats. *Metabolism* 45:865–872, 1996
40. Cameron NE, Gibson TM, Cotter MA: Effects of poly(ADP-ribose) polymerase inhibition in large and small nerve fibre function in experimental diabetes (Abstract). *Diabetologia* 46 (Suppl. 2):A315, 2003
41. Soriano FG, Pacher P, Mabley J, Liaudet L, Szabo C: Rapid reversal of the diabetic endothelial dysfunction by pharmacological inhibition of poly-(ADP-ribose) polymerase. *Circ Res* 89:684–691, 2001
42. Cameron NE, Eaton SE, Cotter MA, Tesfaye S: Vascular factors and metabolic interactions in the pathogenesis of diabetic neuropathy. *Diabetologia* 44:1973–1988, 2001
43. Obrosova I, Cao X, Greene DA, Stevens MJ: Diabetes-induced changes in lens antioxidant status, glucose utilization and energy metabolism: effect of DL-alpha-lipoic acid. *Diabetologia* 41:1442–1450, 1998
44. Obrosova IG, Fathallah L: Evaluation of an aldose reductase inhibitor on lens metabolism, ATPases and antioxidative defense in streptozotocin-diabetic rats: an intervention study. *Diabetologia* 43:1048–1055, 2000
45. Calcutt NA, Allendoerfer KL, Mizisin AP, Middlemas A, Freshwater JD, Burgers M, Ranciato R, Delcroix JD, Taylor FR, Shapiro R, Strauch K, Dudek H, Engber TM, Galdes A, Rubin LL, Tomlinson DR: Therapeutic efficacy of sonic hedgehog protein in experimental diabetic neuropathy. *J Clin Invest* 111:507–514, 2003
46. Obrosova IG, Li F, Abatan OI, Pacher P, Souhan GJ, Szabo C, Stevens MJ: Evaluation of orally active poly(ADP-ribose)polymerase inhibitor in the model of early diabetic neuropathy (Abstract). *Diabetologia* 46 (Suppl. 2):A71, 2003
47. Du X, Matsumura T, Edelstein D, Rossetti L, Zsengeller Z, Szabo C, Brownlee M: Inhibition of GAPDH activity by poly(ADP-ribose) polymerase activates three major pathways of hyperglycemic damage in endothelial cells. *J Clin Invest* 112:1049–1057, 2003
48. Fernyhough P, Gallagher A, Averill SA, Priestley JV, Hounsom L, Patel J, Tomlinson DR: Aberrant neurofilament phosphorylation in sensory neurons of rats with diabetic neuropathy. *Diabetes* 48:881–889, 1999
49. Stevens EJ, Tomlinson DR: Effects of endothelin receptor antagonism with bosentan on peripheral nerve function in experimental diabetes. *Br J Pharmacol* 115:373–379, 1995
50. Pop-Busui R, Marinescu V, Van Huysen C, Li F, Sullivan K, Greene DA, Larkin D, Stevens MJ: Dissection of metabolic, vascular, and nerve conduction interrelationships in experimental diabetic neuropathy by cyclooxygenase inhibition and acetyl-L-carnitine administration. *Diabetes* 51:2619–2628, 2002